Transactions, SMiRT-22
San Francisco, California, USA - August 18-23, 2013
Division IX

AN EXPERIMENTAL STUDY OF THE IN-PLANE RESPONSE OF STEEL-CONCRETE COMPOSITE WALLS

Siamak Epackachi[1], Nam H. Nguyen[1], Efe G. Kurt[2], Andrew S. Whittaker[3], and Amit H. Varma[4]

[1] PhD Candidate, Dept. of Civil, Structural and Environmental Engineering, University at Buffalo, NY (siamakep@buffalo.edu)
[2] PhD Candidate, School of Civil Engineering, Purdue University, IN
[3] Professor and Chair; Director, MCEER; Dept. of Civil, Structural and Environmental Engineering, University at Buffalo, NY
[4] Associate Professor, School of Civil Engineering, Purdue University, IN

ABSTRACT

Steel-concrete (SC) composite walls are being used for the construction of containment internal structures and shielding structures in nuclear power plants. SC walls are composed of steel faceplates, connectors and infill concrete, where the connectors are typically constructed from cross-wall tie rods and shear studs welded to the faceplates. The design of SC walls for safety-related nuclear structures has been based in part on proprietary test data and data available in the literature. Most of the tests conducted to date have been at a relatively small scale and have focused on the *essentially elastic* range of response.

The experimental behavior of four large-size SC walls subjected to cyclic in-plane loading is summarized in this paper. The walls have an aspect ratio of 1 and are flexure critical. A bolted SC wall to RC foundation connection is studied. A focus is the inelastic range of response, which is expected for beyond design basis shaking of nuclear power plant structures. A number of design parameters are investigated, including infill concrete thickness, reinforcement ratio, stud spacing, and tie bar spacing. The pre-test analysis, force-displacement responses, and damage to the steel plates and infill concrete are documented. The walls achieved the peak shear strengths calculated using simplified procedures and ABAQUS. Pinching of the force-displacement response is observed at displacements greater than that associated with peak load. The post-peak load behavior of the walls is affected by the faceplate slenderness ratio.

INTRODUCTION

Steel-concrete (SC) composite walls are being used for the construction of containment internal structures and shielding structures in large light water reactors in the United States and abroad. SC walls have been proposed for other nuclear construction, including small modular reactors. Although the elastic response of SC walls under in-plane loading is reasonable well understood (and just as well understood as reinforced concrete construction), information on post-elastic (inelastic) response is minimal because the focus of nuclear power plant design has been elastic response for design basis earthquake shaking.

The failures at the Fukushima Daiichi nuclear power plant in 2011 and recent initiatives from the US Nuclear Regulatory Commission in the aftermath of the Great East Japan Earthquake in 2011 have emphasized the importance of understanding component and system behavior for earthquake shaking more intense than design basis.

This paper addresses the response of SC walls under beyond design basis loadings. The scope of the experimental program is limited to four specimens. Only in-plane loading is considered. Many additional tests will have to be undertaken to fully understand the seismic response of SC walls through failure under in-plane and out-of-plane loadings and to validate numerical models and tools for the purpose of design and assessment. The following sections of the paper describe the testing program and pre-test analyses, and present key experimental results, damage data, and concluding remarks.

EXPERIMENTAL PROGRAM

Test specimen description

Four large-size specimens (SC1 through SC4) were built and tested under displacement-controlled cyclic loading. The tests were conducted in the NEES laboratory at the University at Buffalo with support from the Bowen Laboratory at Purdue University. The design variables considered in the testing program include reinforcement ratio, tie-rod and stud spacing. The aspect ratio (height-to-length, *H/L*) of all walls was 1.0. Information on the four walls is provided in Table 1. In this table, studs and tie rods serve on connectors, spaced at distance *S*, the overall thickness of the wall is *T*, the thickness of each faceplate is t_p, the reinforcement ratio is $2t_p/T$, and the faceplate slenderness ratio is S/t_p.

Table 1. Test specimen configurations

Specimen	Wall dimension *(H×L×T)* (in.× in.× in.)	Stud spacing (in.)	Tie rod spacing (in.)	Reinforcement ratio (%)	Faceplate slenderness ratio	Day-of-test wall concrete strength (ksi)
SC1	60×60×12	4	12	3.1	21	4.5
SC2	60×60×12	-	6	3.1	32	4.5
SC3	60×60×9	4.5	9	4.2	24	5.3
SC4	60×60×9	-	4.5	4.2	24	5.3

The diameter of the studs and tie rods was 0.375 in. for all walls; the studs and tie rods were fabricated from 50 ksi steel. The yield and ultimate strengths of the steel faceplates calculated from three coupon tests, were 38 and 55 ksi, respectively. The nominal compressive strengths of the infill concrete and the foundation concrete were 4 and 6 ksi, respectively.

Each SC wall was installed on top of a re-usable foundation block. The base of each wall included a 1-in. thick base plate to which the faceplates were CJP groove welded. Two rows of 13 number 0.675-in. diameter studs were welded to the base plate to bond the concrete and improve the transfer of shearing and tensile forces. The base plate was installed atop a 1-in. thick base plate embedded in the foundation block and was secured to the foundation block using 22 1.25-in. diameter threaded B7 bars that were post-tensioned to 100 kips per bar. Figure 1 is a photograph of SC1 installed on the foundation block.

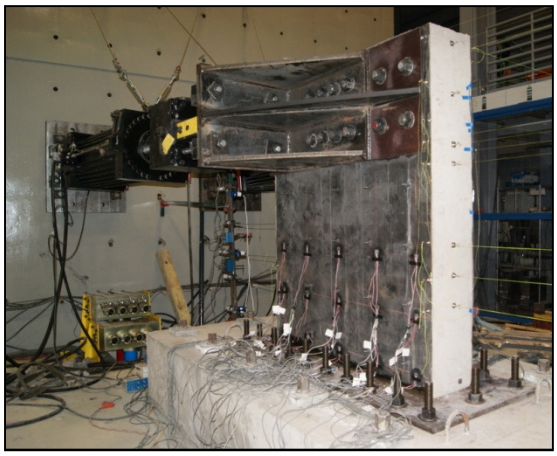

Figure 1. Specimen SC1

Pre-test analysis

Pre-test predictions of the responses of trial SC walls were made to inform the design, detailing and instrumentation of the test specimens, design the re-usable foundation block, and develop a loading protocol. Only those pre-test calculations relevant to SC1 through SC4 are presented below.

Calculations were performed to determine whether specimens were flexure-critical or shear-critical. Nominal material properties were used. The flexural strength of the SC walls was estimated using the cross-section program XTRACT (Chadwell et al. 2002); the corresponding maximum shearing forces were 344 kips and 328 kips for SC1/SC2 and SC3/SC4, respectively. The flexural strength calculation assumed perfect bond between the steel faceplates and the infill concrete. The maximum shearing resistance of the walls was calculated using the draft Appendix N9 to AISC N690 (AISC 2010), Ozaki et al. (2004), and Varma et al. (2011a,b & 2012) to be 870/855/815 kips for SC1/SC2 and 840/855/780 kips for SC3/SC4. The shear resistance calculations assumed shear yielding of the faceplates. These calculations showed the walls to be flexure critical, with a maximum resistance less than the capacity of the actuators proposed for loading the walls.

The general-purpose finite element code ABAQUS (2010) was then used to calculate the shearing force-lateral displacement calculations for the four walls. The concrete damage plasticity (CDP) model was used for the infill and the J2 plasticity model with isotropic hardening was used for the steel faceplates. Friction between the infill concrete and the steel faceplates, and buckling of the steel faceplates were considered. Beam elements were used to represent the studs and tie rods. Solid elements were used to model the infill concrete, foundation block, base plates, loading plates and post-tensioning bars. Shell elements were used for the steel faceplates. The infill concrete was modeled with 1 in × 1 in × 1 in elements and the steel faceplates were modeled with 0.5 in × 0.5 in elements. The model took advantage of symmetry to reduce the computational effort. The ABAQUS model is shown in Figure 2a. Nominal material properties were used for the pre-test ABAQUS calculations.

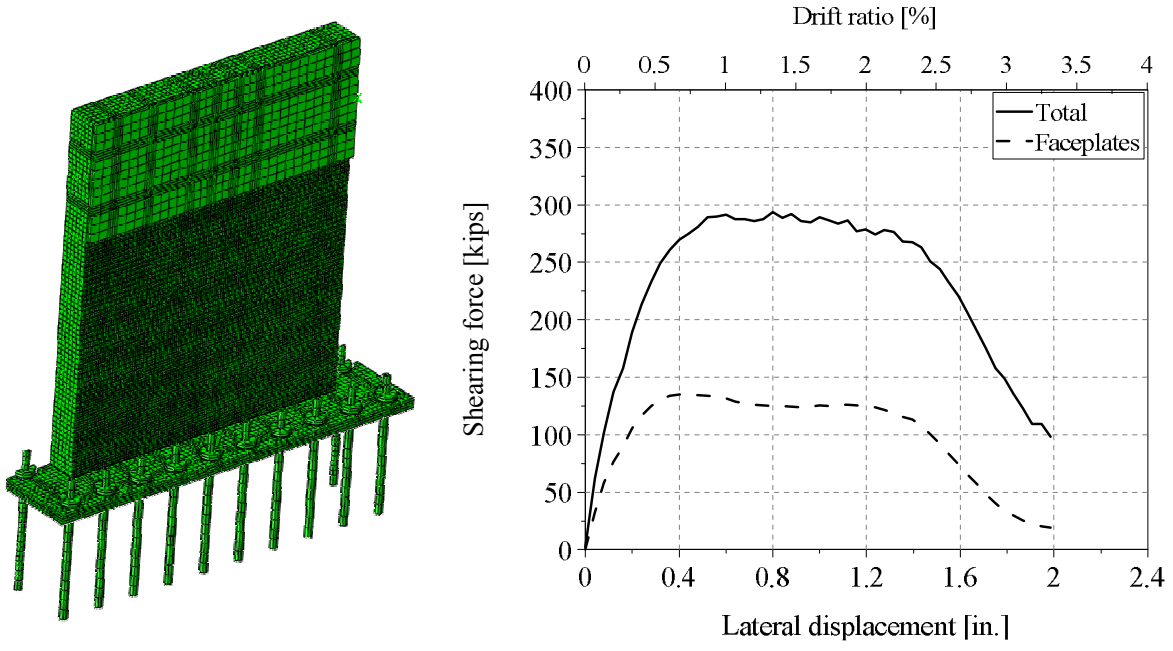

(a) Model (b) Force-displacement relationship

Figure 2. ABAQUS modeling of SC1

The predicted shearing force-lateral displacement relationship of SC1 is presented in Figure 2b. Drift ratio is calculated by dividing the lateral displacement by the vertical distance between the line of loading and the top of the foundation block (=60 inches). The solid black line and the dashed black line represent the total force and the force resisted by the steel faceplates. The peak resistance of 300 kips agrees reasonably well with the estimate of shear corresponding to flexural strength (= 344 kips), which ignores flexure-shear interaction. For SC1, the resistance of the steel faceplates (=135 kips) is approximately 45% of the total resistance, noting that the % resistance of the faceplates will increase as the wall transitions from flexure-critical to shear-critical.

Figure 3 presents the distributions of vertical stress (S22) and shearing stress (S12) in SC1 at peak shearing resistance, in units of ksi. It is evident from these distributions that yielding of the faceplates (and their subsequent buckling and fracture) is affected more by normal stress (S22) than shearing stress, which is an expected result because the walls are flexure-critical.

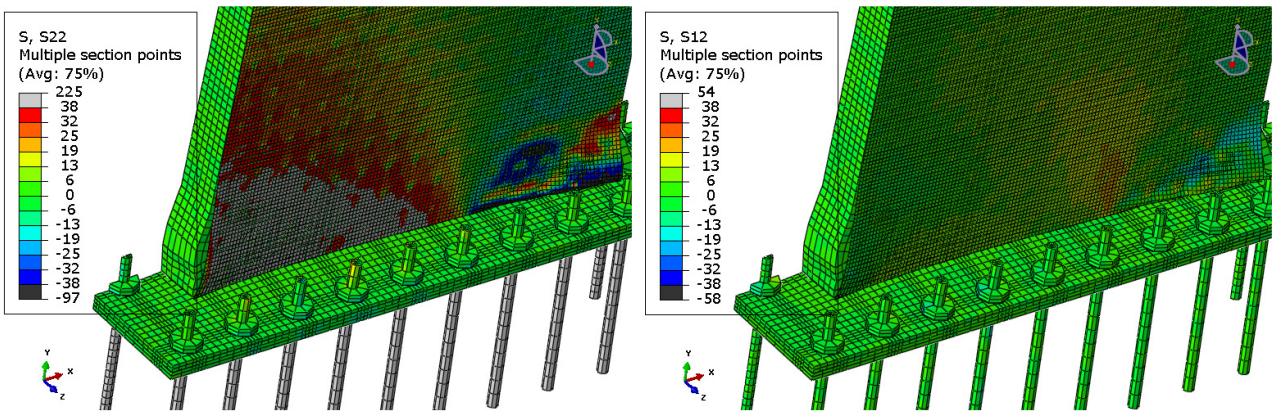

(a) Vertical normal stress (S22) distribution (b) Shear stress (S12) distribution

Figure 3. Stresses in SC1 at the point of maximum resistance

Test setup

Two horizontally inclined high force-capacity actuators were used to apply cyclic lateral loads to the top of the SC walls. The foundation block was post-tensioned to the strong floor with 14 number 1.5 in. diameter Dywidag bars to prevent foundation movement during testing. The test setup is shown in Figure 4.

The displacement-controlled, reversed cyclic loading was based on that proposed by ACI Committee 374. Two cycles of loading were imposed at displacements equal to fractions and multiplies of a reference displacement (=0.14 inch): 0.1, 0.5, 0.75, 1, 2 ... 15, where the calculation of the reference displacement is described in Epackachi (2014). The loading speed was 0.01 in./sec.

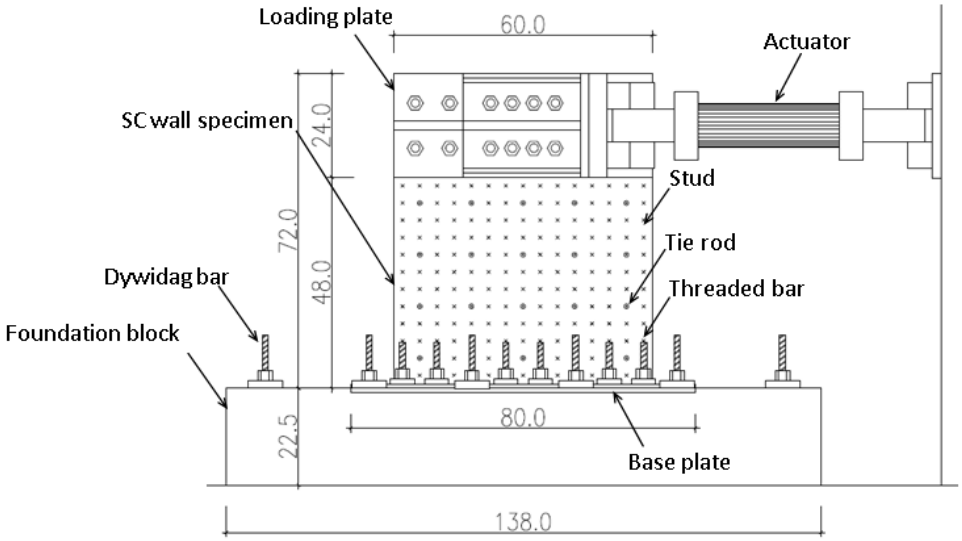

Figure 4. SC wall test setup

Instrumentation

Krypton light emitting diodes (LEDs), rosette strain gages, linear potentiometers, Temposonic displacement transducers, and linear variable displacement transducers were used to collect data. String potentiometers and Temposonics were attached to the ends of the wall to measure the in-plane displacement of the walls. Four string potentiometers measured out-of-plane displacement; one at each corner of the specimen. Linear potentiometers and the Krypton LEDs measured the horizontal and vertical displacements of the foundation block relative to the strong floor.

The Krypton system was used to monitor the 3D displacements of the wall specimens. LEDs were attached to one steel faceplate. Rosette strain gages were installed at three elevations on the other faceplate. The positions of the LEDs and strain gages on SC3 are presented in Figure 5. The applied load was calculated as the sum of the in-plane components of the actuator forces.

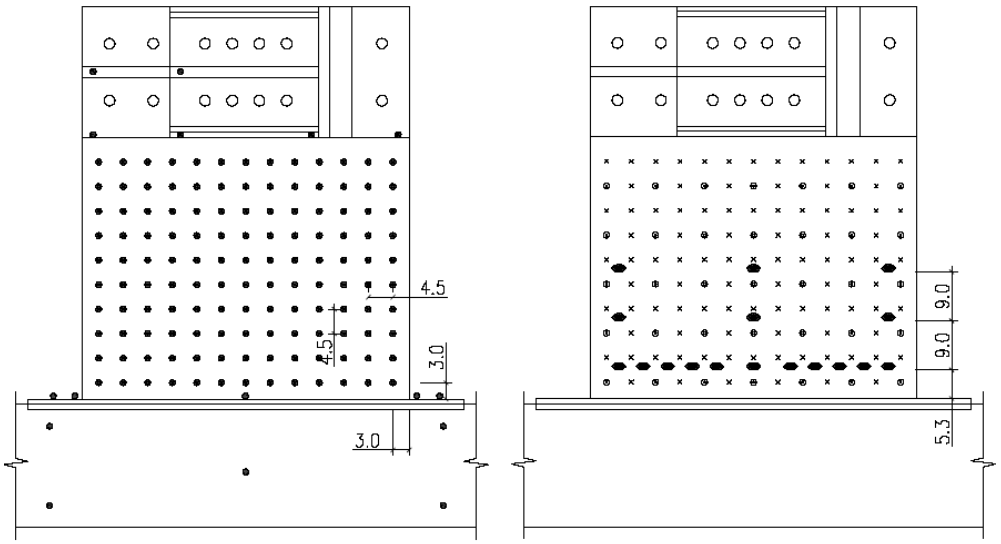

(a) Krypton LEDs (b) Rosette strain gages

Figure 5. Krypton LEDs and strain gages on SC3

EXPERIMENTAL RESULTS

Key test results are provided in Table 2 and Figure 6. The initial stiffness of SC1 is greater than that for SC2 through SC4, where values were calculated at drift angles less than 0.02%. The values of the displacements corresponding to the onset of faceplate buckling are listed in column 3. Columns 4 and 5 in the table present computed data for the onset of faceplate yielding, where forces and displacements are calculated using rosette strain gage data and assuming a Von Mises yield criterion. Columns 6 and 7 present peak loads and the corresponding drift angles in the first (positive) and third (negative) quadrants (see Figure 6). Column 8 lists the drift angles at 80% of the peak load in the first and third quadrants.

Table 2. Results summary for SC1 through SC4

Specimen	Initial stiffness (kips/in.)	Data point					
		Onset of steel plate buckling	Onset of steel plate yielding		Peak load		Drift angle at 80% peak load (%) Pos/Neg
		Drift angle (%)	Load (kips)	Drift angle (%)	Load (kips) Pos/Neg	Drift angle (%) Pos/Neg	
SC1	1680	0.48	240	0.48	317/320	1.18/1.18	2.42/2.56
SC2	1240	0.48	200	0.48	314/319	1.18/1.18	1.85/1.74
SC3	1380	0.70	185	0.48	265/275	1.40/1.18	1.69/1.88
SC4	1310	0.70	200	0.48	270/275	1.18/1.18	1.94/2.40

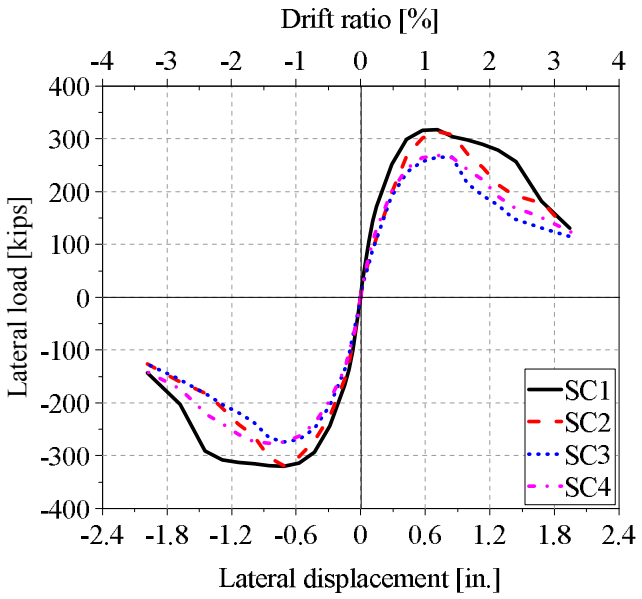

Figure 6. Cyclic backbone curves for the SC walls

The initial stiffness of SC3 and SC4 was less than that of the thicker SC1. The initial stiffness of SC2 was substantially less than SC1, which was not expected and is attributed to flexibility at the base of the wall. Buckling of the faceplates occurred at their free edges prior to achieving peak load, noting that studs were not provided at the vertical free edges. Plate buckling extended towards the center of wall during subsequent cycles of loading and was affected by the connector spacing as seen in Figure 7.

Yielding of the faceplates occurred prior to peak load. Peak load was observed at a relatively high drift angle of 1.1+%. The peak loads developed in SC1 and SC2, and SC3 and SC4 are similar, which indicates that connector spacing in the range provided does not impact the peak shearing resistance in flexure-critical walls. The peak loads in SC1 and SC2 are greater than SC3 and SC4 because the infill concrete in SC1 and SC2 is 3 inches thicker. The drift angle at 80% of peak load provides some insight into the importance of the connector spacing (or faceplate slenderness ratio). Given that the walls sustained their peak loads at the same drift angle of 1.18% (7 of 8 per Table 2), the greater the drift angle at 80% peak load, the slower the deterioration of strength with increasing displacement. Wall SC1 had the smallest slenderness ratio of 21 and the greatest drift angle at 80% peak load.

The cyclic backbone curves of Figure 6 provide further insight into the behavior of these flexure-critical walls. Consider SC1 and SC2, which sustained a similar peak load. The rate of strength deterioration in SC2 post peak load is much greater than in SC1 up to a drift angle of approximately 2.5%, which is attributed directly to faceplate slenderness. Consider SC3 and SC4, which had identical faceplate slenderness: the rate of strength degradation post peak load in the two walls is virtually identical. The load in all four walls at a drift angle of 3.3% was approximately 130 kips. The reason for the more rapid drop in strength of the two thicker walls at the higher drift angles is not yet understood and is being studied at this time.

Damage to SC walls

Figure 7 provides photographs of damage to SC2. The damage progression in the four SC walls was identical, namely 1) tensile cracking of the concrete at both ends of the wall, 2) outward buckling and yielding of the steel faceplates at the base of the wall, and 3) tearing of the steel faceplates along their welded connection to the base plate. Tearing of the faceplates initiated at drift angles of 1.4% for SC2 and 1.6% for SC1, SC3, and SC4, respectively.

A steel faceplate was removed from each of two specimens, SC2 and SC4, for the purpose of documenting damage to the infill concrete. As seen in Figure 7a, one wide diagonal crack formed in the infill concrete and most of the damage to the infill was concentrated immediately above the base plate, at the level of the first row of tie rods. It is unknown whether the row of connectors immediately above the baseplate represents a potential failure plane, which would have to be addressed in design standards through prescriptive detailing. (On-going numerical studies will investigate this issue.)

(a) Infill concrete (b) SC wall

Figure 7. Damage to SC2 at 3.3% drift angle

Load-displacement cyclic response

The load-displacement relationships for SC1 through SC4 are shown in Figure 8. The load displacement relationships are similar, with higher peak strengths in the two thicker walls. Pinched hysteresis loops and loss of strength and stiffness are observed for all walls, but occurred at displacements greater than that corresponding to peak strength. The pinching and strength degradation are attributed to faceplate buckling, cracking and crushing of infill concrete, and tearing of the steel faceplate immediately above the baseplate.

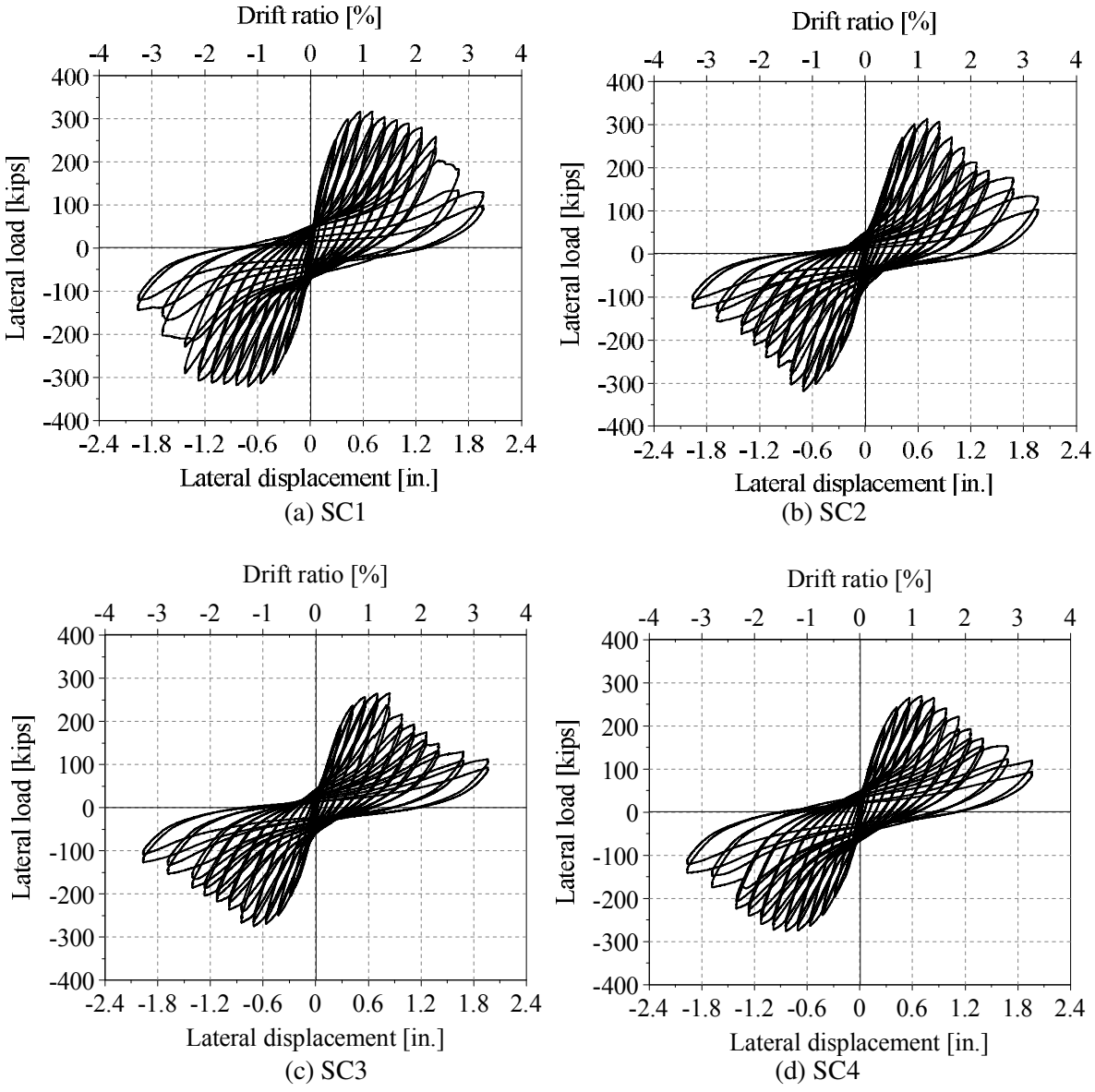

Figure 8. Lateral load - displacement relationships of SC walls

Initial stiffness

Initial stiffness is an important parameter for the analysis of structural systems incorporating SC walls. The measured and predicted values of initial stiffness for all tested SC walls are presented in Table 3. Column 2 provides the measured initial stiffness of SC walls, where the values were calculated at drift angles of 0.02%. To investigate the effect of foundation flexibility, two sets of ABAQUS models of the SC walls were prepared and analyzed: 1) including all components of the base connection and foundation block, and 2) assuming a rigid connection of the walls to an infinitely stiff base. The ABAQUS predictions of initial stiffness accounting for foundation flexibility predict the measured values very well. The assumption of a rigid base, which would be commonly made by practitioners, would lead to an overestimation of the initial stiffness by a factor of nearly 3.

Table 3. Values of measured and predicted stiffness for SC1 through SC4

Specimen	Measured initial stiffness (kips/in.)	ABAQUS predictions	
		Rigid base (kips/in.)	Flexible base (kips/in.)
SC1	1680	4310	1550
SC2	1240	4300	1500
SC3	1380	4170	1260
SC4	1310	4100	1390

CLOSING REMARKS

Four large-scale SC walls (SC1 through SC4) were constructed at the NEES facility at the University at Buffalo as part of a NSF-funded NEES project on low aspect ratio conventional and composite shear walls. The walls had an aspect ratio of 1.0 and were flexure critical. The walls were tested under reversed cyclic loading. The design space for the walls included reinforcement ratio and faceplate slenderness ratio. A bolted baseplate to RC foundation connection was used for all four walls.

The key findings of this study to date are:

1. The four flexure-critical walls sustained peak loads close to that predicted by pre-test calculations using commercially available software. Faceplate slenderness ratio did not influence the peak resistance of the walls, for the range of slenderness ratio studied (21 to 32).
2. The damage progression in the four walls was identical, namely cracking and crushing of infill concrete at the toes of the walls, outward buckling and yielding of the steel faceplates near the base of the wall, and tearing of the faceplates at their junction with the base plate. Buckling of the faceplates would have been delayed if a vertical row of studs had been provided near the boundaries of the walls.
3. Pinched hysteresis and loss of stiffness and strength was observed in all four walls at lateral displacements greater than that corresponding to peak load.
4. The damage to the infill concrete was concentrated in the region immediately above the baseplate and at and below the first row of connectors in all four walls.
5. The post-peak response of flexure-critical SC walls is influenced by faceplate slenderness ratio, with a smaller rate of degradation post peak load observed in the wall with the smallest faceplate slenderness ratio.
6. Numerical studies of initial stiffness showed the importance of addressing foundation flexibility. Including foundation flexibility enabled the ABAQUS calculations of initial stiffness to match the

measured values well. Ignoring the foundation flexibility would lead to an overestimation of the initial stiffness by a factor of 3, which would have a significant impact on the computations of demand on structural components and safety-related secondary systems.

ACKNOWLEDGEMENTS

This project was supported in part by the US National Science Foundation under Grant No. CMMI-0829978. This support is gratefully acknowledged. We also thank the technical staff of the NEES laboratory at the University of Buffalo, and the Bowen Laboratory at Purdue University, and LPCiminelli Inc. for their contributions to the project.

REFERENCES

ABAQUS. (2010), *ABAQUS User's Manual*, Version 6.10, Hibbitt, Karlsson & Sorensen, Inc., Pawtucket, RI.

AISC. (2010). "Specification for Design of Steel-Plate Composite (SC) Walls in Safety-Related Structures for Nuclear Facilities", *AISC Proposal APPENDIX N9*, Chicago, IL.

Epackachi, S. (2014). "Numerical and experimental studies on steel-concrete composite walls, " *Ph.D. Dissertation in preparation*, Department of Civil, Structural and Environmental Engineering, University at Buffalo.

Chadwell, C. B., and Imbsen, R. A. (2002), "XTRACT-cross section analysis software for structural and earthquake engineering", TRC, Rancho Cordova, CA, http://www.imbsen.com/xtract.htm.

Ozaki, M., Akita, S., Osuga, H., Nakayama, T., and Adachi, N. (2004). "Study on steel plate reinforced concrete panels subjected to cyclic in-plane shear," *Nuclear Engineering and Design*, 228(1-3), 225–244.

Varma, A. H., Malushte, S. R., Sener, K., Lai, Z. (2011a). "Steel-plate composite (SC) walls for safety related nuclear facilities: design for in-plane and out-of-plane demands," *Proceedings of the 21st IASMiRT Conference (SMiRT 21)*, New Delhi, India, Paper ID #760.

Varma, A.H., Zhang, K., Chi, H., Booth, P. and Baker, T. (2011b). "In-plane shear behavior of SC composite walls: theory vs. experiment," *Proceedings of the 21st IASMiRT Conference (SMiRT 21)*, New Delhi, India, Paper ID #764.

Varma, A. H., Malushte, S. R., Sener, K. C., and Booth, P. N. (2012). "Analysis recommendations for steel-composite (SC) walls of safety-related nuclear facilities," *Structures Congress*, ASCE, 1871–1880.